BJR

https://doi.org/10.1259/bjr.20210837

Received: 12 July 2021 | Revised: 21 October 2021 | Accepted: 17 November 2021

Cite this article as:
Takahashi H, Kashiwagi N, Arisawa A, Matsuo C, Kato H, Adachi H, et al. Imaging of the nigrostriatal system for evaluating the preclinical phase of Parkinson's disease development: the utility of neuromelanin, diffusion MRI, and DAT-SPECT. *Br J Radiol* 2022; **95**: 20210837.

## FULL PAPER

# Imaging of the nigrostriatal system for evaluating the preclinical phase of Parkinson's disease development: the utility of neuromelanin, diffusion MRI, and DAT-SPECT

**[1,2]HIROTO TAKAHASHI, MD, [3]NOBUO KASHIWAGI, MD, PhD, [2]ATSUKO ARISAWA, MD, [2]CHISATO MATSUO, MD, [4]HIROKI KATO, MD, [5]HIROYOSHI ADACHI, MD, [6]YUTA KAJIYAMA, MD, [6]HIDEKI MOCHIZUKI, MD, PhD and [2]NORIYUKI TOMIYAMA, MD, PhD**

[1]Division of Health Sciences, Osaka University Graduate School of Medicine, Suita, Japan
[2]Department of Diagnostic and Interventional Radiology, Osaka University Graduate School of Medicine, Osaka, Japan
[3]Department of Future Diagnostic Radiology, Osaka University Graduate School of Medicine, Osaka, Japan
[4]Department of Nuclear Medicine and Tracer Kinetics, Osaka University Graduate School of Medicine, Osaka, Japan
[5]Department of Psychiatry, Osaka University Graduate School of Medicine, Osaka, Japan
[6]Department of Neurology, Osaka University Graduate School of Medicine, Osaka, Japan

Address correspondence to: Dr Hiroto Takahashi
E-mail: *hiroto.takahashi07@gmail.com*

**Objective:** To assess the utility of examining the nigrostriatal system with MRI and dopamine transporter (DAT) imaging for evaluating the preclinical phase of Parkinson's disease (PD).
**Methods:** The subjects were 32 patients with early PD and a history of probable rapid eye movement sleep behavior disorder (RBD; PD group), 15 patients with idiopathic RBD (RBD group), and 24 age-matched healthy controls (HC group) who underwent neuromelanin and diffusion tensor MRI for analysis of the substantia nigra pars compacta (SNpc). The RBD and PD groups underwent DAT imaging. In the RBD group, totals of 39 MRI and 27 DAT imaging examinations were obtained longitudinally. For each value, intergroup differences and receiver operating characteristic analysis for diagnostic performance were examined statistically.
**Results:** The neuromelanin value was significantly lower and the diffusion tensor values except fractional anisotropy were significantly higher in the RBD and PD groups than in the HC group. The DAT specific binding ratio (SBR) was significantly lower in the PD group than in the RBD group. The areas under the receiver operating characteristic curves (AUCs) for neuromelanin/mean diffusivity value in the SNpc were 0.76/0.82 for diagnosing RBD and 0.83/0.80 for diagnosing PD. The area under the receiver operating characteristic curves for the SBR for discriminating PD from RBD was 0.87.
**Conclusion:** MRI and DAT imaging may be useful for evaluating sequential nigrostriatal changes during the preclinical phase of PD.
**Advances in knowledge:** MRI detects nigrostriatal changes in both RBD and early PD, and DAT imaging detects nigrostriatal changes during the transition to PD in RBD.

## INTRODUCTION

In the preclinical phase of Parkinson's disease (PD), neuropathological features develop in the central nervous system, but they do not reach the threshold for clinical symptoms to emerge or for a diagnosis to be established. Because therapeutic intervention might be most successful when provided in this preclinical disease phase, it is a clinical and research priority to identify neurodegenerative changes in the preclinical phase of PD.[1] Rapid eye movement (REM) sleep behavior disorder (RBD) is characterized by dream-enacting behaviors that are linked to REM sleep without atonia.[2] RBD is a prodromal synucleinopathy that is commonly associated with the development of PD, dementia with Lewy bodies (DLB), or multiple system atrophy.[3]

Neuroimaging of the nigrostriatal system has recently been reported as useful in the diagnosis of both RBD and PD. This study is used to examine two main regions within the nigrostriatal system, the substantia nigra pars compacta (SNpc) and the striatum. For SNpc analysis, neuromelanin-sensitive MRI is a novel technique that enables direct

visualization of neuromelanin-containing neurons in the SNpc.[4] Previous studies reported that neuromelanin-sensitive MRI shows a significant reduction of signal intensity in the SNpc in patients with PD and even in patients with early PD.[5] Another report indicated that neuromelanin-sensitive MRI can enable detection of substantia nigra (SN) damage in RBD with good diagnostic accuracy.[6] Diffusion tensor imaging (DTI) is an MRI technique that measures water diffusion and can be used to quantify microstructural changes in brain tissue. DTI has been applied successfully to various neurodegenerative disorders, and a DTI study has described the specific microanatomic alterations in the SN of RBD.[7] Analysis of the nigrostriatal system, using the latest advanced diffusion-weighted MRI technique, neurite orientation dispersion and density imaging (NODDI), has demonstrated PD-related neuron loss in both the SNpc and putamen in the striatum.[8] The results of a diffusion-weighted MRI analysis of the entire nigrostriatal system in PD showed that dopamine neurodegeneration occurs in both the presynaptic terminals and the distal nigrostriatal pathway.[9] Striatal imaging appears to also be useful for evaluating the early stages of PD. Dopamine transporter (DAT) is a protein located in the presynaptic membrane on terminals of dopaminergic projections from the SN to the striatum, and it provides a marker of dopamine terminal innervation. Iodine-123-labeled 2β-carbomethoxy-3β-(4-iodophenyl) tropane single-photon emission computed tomography ($^{[123I]}$-CIT SPECT) is a functional neuroimaging tool that can be used to evaluate *in vivo* the integrity of the nigrostriatal dopamine system.[10] In PD and DLB, DAT-SPECT detects reduced tracer uptake in the striatum. A previous study reported that DAT-SPECT detected a decrease in striatal tracer uptake indicative of progressive nigrostriatal dopaminergic dysfunction in RBD.[11]

These studies suggest that the SNpc and the striatum may be most sensitive to changes in the nigrostriatal system in PD and in RBD, its precursor. Therefore, we postulated that a comprehensive neuroimaging technique that analyzed both the starting point (the SNpc) and the terminus (the striatum) might show sequential structural and functional changes in the nigrostriatal system during the preclinical phase of PD, which could provide a high diagnostic potential for both RBD and early PD, as well as the transition from RBD to PD. The aim of this study was to assess the utility of examining the nigrostriatal system with MRI and DAT-SPECT for evaluating the preclinical phase of PD and to explore an imaging biomarker for the development of PD.

## METHODS AND MATERIALS

Our Institutional Review Board approved this study, and all participants provided written, informed consent.

### Patients and controls

This retrospective study included 103 patients with early PD who were diagnosed with PD between September 2014 and July 2020. To assess sequential dopamine neuronal changes in the nigrostriatal system during the entire preclinical phase of PD, including the RBD state, patients with a history of probable RBD were chosen from among patients with early PD. The patients were diagnosed by experienced neurologists (YK and HM, with 10 and 30 years of experience in movement disorders, respectively) using the UK Parkinson's Disease Society Brain Bank criteria.[12] Disease severity was assessed using the Hoehn and Yahr (HY) scale.[13] Early PD was defined as HY Stage 1 or 2. Probable RBD was defined as a score ≥5 on the Japanese v. of the RBDSQ-J RBD screening questionnaire.[14] According to the inclusion and exclusion criteria (Figure 1), 32 patients met the criteria for PD (PD group: 13 women, 19 men; age, 66.01 ± 10.02 years). All patients were taking anti-PD medications such as levodopa or dopamine agonists at the time of MRI and clinical examination. 1 year after diagnosis, all patients remained free of other parkinsonism and continued to respond satisfactorily to anti-PD therapy.

Idiopathic RBD was diagnosed by an experienced psychiatrist (HA with 20 years of experience) according to the standard guidelines of the International Classification of Sleep Disorders, third edition.[15] A total of 15 patients met the criteria for idiopathic RBD (RBD group; 11 women, 4 men; age, 72.1 ±

Figure 1. Inclusion and exclusion criteria for the PD group. PD, Parkinson's disease; RBD, rapid eye movement sleep behavior disorder.

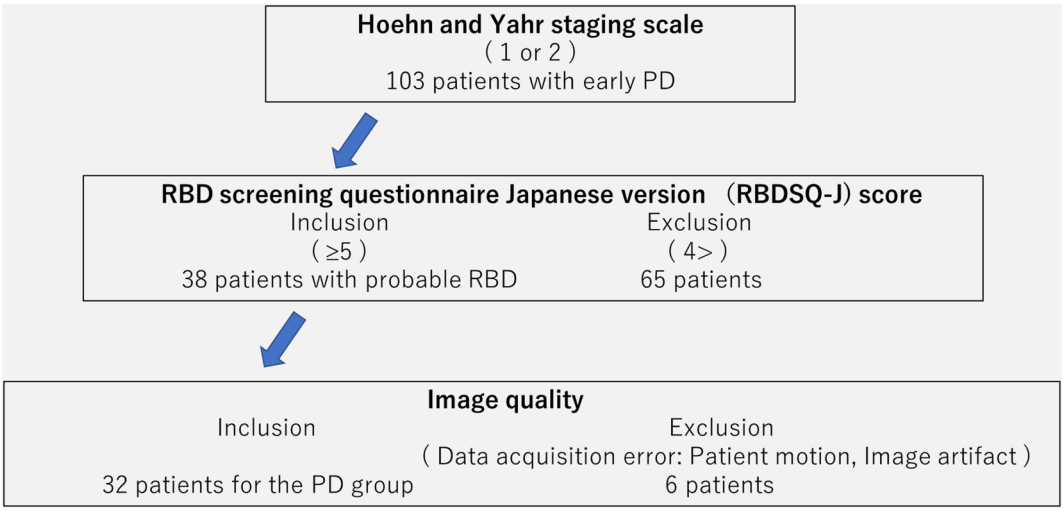

Table 1. Demographics and clinical status of the study participants

| | HC group | RBD group | PD group | *p*-value |
|---|---|---|---|---|
| Female/male (n) | 12/12 | 11/4 | 13/19 | |
| Age (y) | 67.14 ± 4.75 | 72.1 ± 7.29 | 66.01 ± 10.02 | 0.77 |
| HY staging scale score | NA | NA | 1.88 ± 0.32 | |
| Disease duration (y) | NA | 6.39 ± 7.24 | 7.72 ± 4.40 | 0.26 |
| UPDRS part III score | NA | 4.28 ± 3.77 | 23.69 ± 11.33 | 6.15 × 10–5 |
| MMSE | 28.57 ± 1.60 | 28.78 ± 1.09 | 26.38 ± 3.34 | 0.28 |

HC, healthy control; MMSE, Mini-Mental State Examination; NA, not applicable; PD, Parkinson's disease; RBD, rapid eye movement sleep behavior disorde; UPDRS, Unified Parkinson's Disease Rating Scale.
Note. Except where indicated, data are means ± standard deviations.

*p* values in age and MMSE were calculated with analysis of variance with Tukey's post hoc test. *p* values in disease duration and UPDRS part III score were calculated with Wilcoxon signed-rank test.

UPDRS part III score was significantly higher in the PD group than in the RBD group. There were no significant differences among the groups in age, disease duration and MMSE.

7.29 years). The diagnosis of RBD required a history of dream-enacting behaviors in the form of video-polysomnographic demonstration of increased electromyographic activity during REM sleep that was associated with abnormal behaviors. Patients were not taking anti-PD medications. The healthy control (HC) group comprised 24 age-matched healthy volunteers (12 men, 12 women; age, 67.14 ± 4.75 years) who were assessed by experienced neurologists (YK and HM) as having no evidence of any neurodegenerative disorder. The detailed demographic and clinical data of each group are listed in Table 1.

## Imaging studies

All three groups underwent MRI, and the RBD and PD groups underwent DAT-SPECT within 1 month after diagnosis. The HC and PD groups underwent imaging at a single time point. As a longitudinal yearly follow-up study in the RBD group, nine subjects underwent multiple MRI examinations (2–5 times), and eight subjects underwent multiple DAT-SPECT examinations (2–5 times). In total, 39 MRI and 27 DAT-SPECT examinations were performed in the RBD group during the study period. (A detailed schedule of the timing of MRI and DAT-SPECT examinations in the RBD group is provided in the Supplementary Material 1.) A previous RBD study reported that there was no significant difference in the SN between idiopathic RBD subjects and the same subjects at 5 year follow-up,[16] which indicated that there might be only a few changes in the nigrostriatal system during the time course of RBD. Therefore, all imaging data of idiopathic RBD subjects were included as the RBD group in analysis. All subjects in the PD group underwent both MRI and DAT-SPECT.

## MRI

All MRI studies were performed using a 3 T system (Discovery MR750; GE Healthcare, Milwaukee, WI) with a 32-channel receive-only phased-array head coil. DTI was performed using single-shot fat-saturated spin echoplanar imaging (EPI) with the following settings: repetition time/echo time, 12,000/61.3 ms; slice thickness, 2.6 mm; matrix, 128 × 128; field of view, 240 mm; number of excitations, 1; and 15 diffusion gradient directions with $b$ = 1000 s/mm$^2$. Image processing was completed using the diffusion tools in the FSL v. 4.0.1 software package (http://www.fmrib.ox.ac.uk/fsl/).[17] DTI processing comprised affine registration to reduce the effects of eddy currents and calculation of the diffusion tensor parametric maps of mean diffusivity (MD), axial diffusivity (AD), radial diffusivity (RD), and fractional anisotropy (FA). Neuromelanin imaging was performed using $T_1$ weighted fast spin echo (FSE) sequences (repetition time/echo time, 550/10.49 ms; slice thickness, 2.4 mm; flip angle, 180° with no intersection gaps; acquisition matrix, 256 × 256; field of view, 180 mm), because high-resolution $T_1$ weighted FSE images obtained at 3 T can depict the neuromelanin-generated signals by virtue of the synergistic effects of a high signal-to-noise ratio (SNR), high spatial resolution, and signal suppression of the surrounding brain tissue without magnetization transfer effects by T1 prolongation at a high magnetic field.[4] Three-dimensional (3D) sections of a $T_1$ weighted fast spoiled gradient echo sequence were obtained in the sagittal orientation as 1-mm-thick sections (repetition time/echo time, 7.20/2.75 ms; inversion time, 400 ms; flip angle, 11° with no intersection gaps; acquisition matrix, 256 × 256; field of view, 240 mm), which were adapted for using voxel-based morphometric image analysis. In addition to these imaging approaches, axial $T_2$ weighted imaging was performed using FSE sequences (repetition time/echo time, 5800/98.6 ms; slice thickness, 5 mm; flip angle, 111°; acquisition matrix, 320 × 320; field of view, 254 mm) for all subjects as part of their screening or routine clinical care to confirm that there were no other structural abnormalities.

## DAT-SPECT

DAT-SPECT was acquired using a SPECT/CT scanner (Symbia T6 and Symbia Intevo6; Siemens Healthcare, Hoffman Estates, IL) with the following conditions: acquisition duration, 28 min (mid-scan time of around 4 h after [$^{123}$I]-FP-CIT injection); SPECT matrix, 128 × 128 with 128 slices; and acquisition mode, dynamic mode with circular rotation of the gamma camera over

Figure 2. Automatic ROI selection method. We developed a method comprising two steps. First, a preprocessing step that included image coregistration, spatial normalization, and smoothing for all image data; and spatial normalization with a region-focused modification condition performed for each analysis of the SNpc and the striatum. Second, a regional ROI was set on the target region on each image with high reproducibility. SNpc and striatum ROIs were created based on the averaged preprocessed neuromelanin MRI and 3D $T_1$ weighted images of healthy people, respectively. 3D, three-dimensional; DTI, diffusion tensor imaging; DAT, dopamine transporter; ROI, region of interest; SNpc, substantia nigra pars compacta.

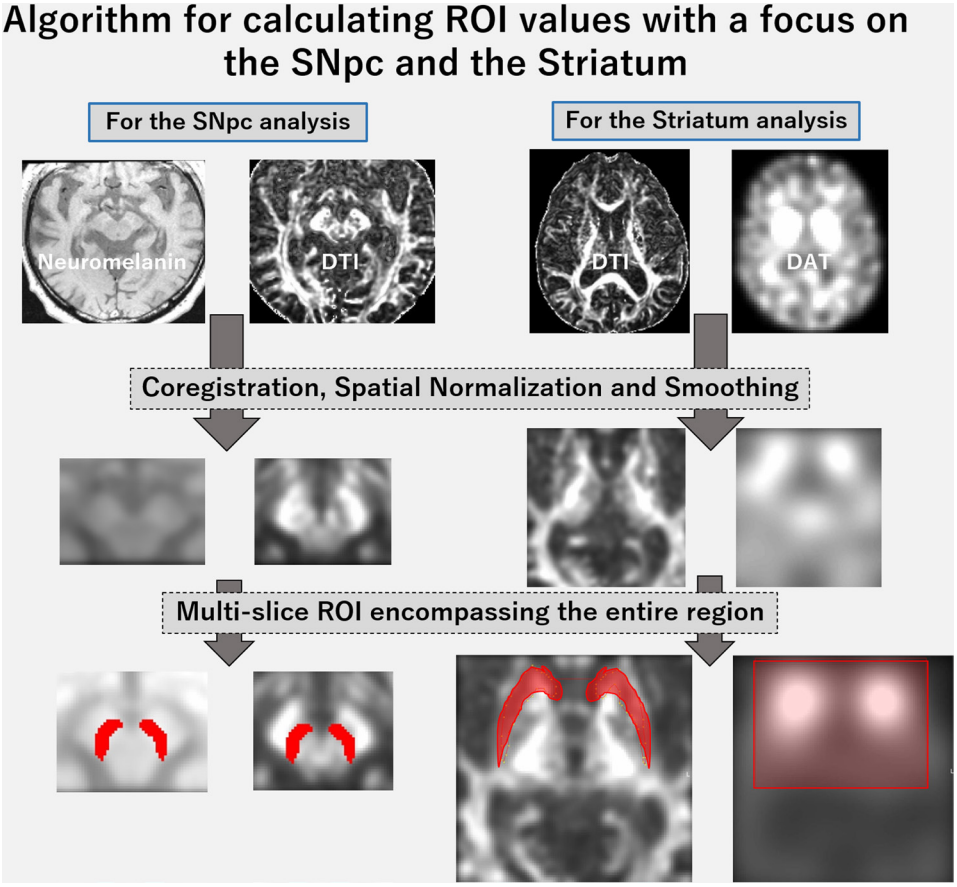


a 360° range in 4°-angular steps (90 views, 210 s/cycle and eight repeats).

## Image analysis

All image data were transferred to a computer. One neuroradiologist (HT) with 18 years of experience who was blinded to the clinical details performed all image processing and analysis. The SNpc and the striatum were chosen for analysis of the target region within the nigrostriatal system. To ensure highly reproducible image analysis of each SNpc and striatum, a customized region of interest (ROI)-based automated segmentation system was developed using a voxel-based morphometric technique to calculate the image values. The algorithm used to calculate each value is shown in Figure 2. The images were preprocessed as follows. All diffusion tensor and neuromelanin MR images and DAT-SPECT images were coregistered with 3D $T_1$ weighted structural images and then spatially normalized to 1 mm voxel size using Statistical Parametric Mapping 12 software and code written in MATLAB R2017a (MathWorks, Natick, MA). The preprocessing provided highly reproducible measurements with the multislice ROI set automatically to cover the entire region of each SNpc and striatum. Because of differences in the size of the target region and in the spatial resolution of the images, the spatially normalized MR images of all subjects were smoothed to remove image noise using an isotropic 4 mm full-width Gaussian kernel, and the spatially normalized DAT-SPECT images of all subjects were smoothed to remove image noise using an isotropic 12 mm full-width Gaussian kernel.

An ROI was then set for each of the SNpc and the striatum using commercially available software (NordicICE v3.3.12; Nordic Imaging Lab, NIL, Bergen, Norway). The SNpc ROI for all images was created by manual segmentation based on the high-intensity area in the bilateral SNpc on the averaged preprocessed neuromelanin images of healthy people. The striatum ROI for diffusion tensor images was created by manual segmentation of the bilateral striatum on the averaged preprocessed 3D T1 images of healthy people. The cubic striatum ROI for DAT-SPECT images was created according to the averaged preprocessed 3D T1 images of healthy people. In the SNpc ROIs, the diffusion tensor values of MD, AD, RD, and FA were measured in $mm^3/s$, and the neuromelanin value was measured in $mm^3$. The analysis of neuromelanin measured the SNpc volume, which has a higher SNR compared with the background region (tegmentum in the

midbrain, which contains no neuromelanin). The SNR of the SNpc in the neuromelanin images was calculated based on the mean values of the automatically segmented background region. Analysis of the DAT-SPECT images was performed by calculating the striatal specific-binding ratio (SBR) based on the mean value of the background region (the occipital lobe for SBR). In measurements of the striatum ROI values, both the diffusion tensor values of MD, AD, RD, and FA and the SBR were used.

### Data analysis

For all diffusion tensor and neuromelanin values of the SNpc and all diffusion tensor values of the striatum, intergroup differences of all groups were identified using analysis of variance with Tukey's post hoc test. For all SNpc and striatum values including SBR, intergroup differences between the RBD and PD groups were identified using the Mann–Whitney *U* test. (Additionally, a statistical longitudinal analysis was performed for the cases of the RBD group who underwent examinations more than three times during the study period. First, longitudinal yearly changes of all image data in each case were calculated. Next, the differences in yearly changes of the cases were assessed using analysis of variance with Tukey's post hoc test. The results are shown in the Supplementary Material 1.) Correlations were assessed between each diffusion tensor value and the neuromelanin value within the SNpc, and between the SNpc value and the striatum value using Pearson's correlation analysis. Receiver operating characteristic (ROC) analysis was used for statistical evaluation of the diagnostic performance of each value for identifying RBD and early PD, as well as for discriminating PD from RBD.

## RESULTS

Regarding each SNpc and striatum value of all groups, Table 2 lists the diffusion tensor and neuromelanin values for the SNpc, and the diffusion tensor values and the SBR for the striatum. For the SNpc, the neuromelanin value was significantly lower in both the RBD and PD groups than in the HC group ($p < 0.001$). The MD, AD, and RD values were significantly higher in the RBD and the PD groups than in the HC group ($p < 0.002$). The FA value did not differ significantly between groups ($p = 0.232$). For the striatum, the MD value did not differ significantly between groups. The AD value was significantly higher in the PD group than in the HC group ($p = 0.047$), and the RD value was significantly lower in the RBD group than in the HC group ($p = 0.025$). The FA value was significantly higher in the RBD group than in the HC group ($p = 0.038$). Regarding intergroup differences between the RBD and PD groups, only the SBR was significantly lower in the PD group than in the RBD group ($p < 0.0001$). These results are presented as graphs in Figures 3 and 4.

Each SNpc and striatum value of the RBD group showed no apparent tendency during the time course of RBD, and the standard deviation of each value was almost the same or smaller, compared to that of the HC and PD groups. (Tables and graphs show no significant sequential changes in all image values of the RBD group in the Supplementary Material 1.)

For the SNpc, a significant negative correlation ($r = -0.43$) was found between the neuromelanin value and the MD value for all groups combined. Because each AD and RD value had a similar relationship to the MD value, and there was no intergroup difference in terms of the FA value, the correlation between these values and the neuromelanin value was not assessed. Except for the RD value, significant correlations were found between the SNpc and the striatum diffusion tensor values for all groups combined. The coefficient of the correlation between the SNpc and the striatum was 0.26 for the MD value, 0.27 for the AD value, 0.20 for the RD value, and 0.56 for the FA value. (These relationships are shown in the Supplementary Material 1.)

ROC analysis quantified the diagnostic performance for each SNpc and striatum value (Figure 5). For the SNpc, the respective areas under the ROC curves (AUCs) for the neuromelanin, MD, AD, RD, and FA values were 0.76 [95% confidence interval (CI): 0.64 to 0.86], 0.82 [95% CI: 0.70 to 0.91], 0.85 [95% CI: 0.74 to 0.93], 0.77 [95% CI: 0.65 to 0.87], and 0.63 [95% CI: 0.49 to 0.74] for RBD; and 0.83 [95% CI: 0.71 to 0.92], 0.80 [95% CI: 0.67 to 0.89], 0.78 [95% CI: 0.64 to 0.88], 0.79 [95% CI: 0.66 to 0.89], and 0.55 [95% CI: 0.41 to 0.69] for early PD. The AUC for the SNpc values for discriminating PD from RBD was not calculated because none of the SNpc values differed significantly between

Table 2. SNpc and striatum values

| SNpc | Neuromelanin value ($mm^3$) | MD ($x10^3$ $mm^2/s$) | AD ($x10^3$ $mm^2/s$) | RD ($x10^3$ $mm^2/s$) | FA ($mm^2/s$) |
|---|---|---|---|---|---|
| HC | $1001.98 \pm 43.72^{*+}$ | $861.88 \pm 84.08^{*+}$ | $1295.36 \pm 130.59^{*+}$ | $645.79 \pm 68.36^{*+}$ | $0.47 \pm 0.04$ |
| RBD | $960.21 \pm 51.38^{*}$ | $960.69 \pm 83.80^{*}$ | $1442.21 \pm 107.53^{*}$ | $721.15 \pm 79.91^{*}$ | $0.49 \pm 0.04$ |
| PD | $935.95 \pm 60.50^{+}$ | $981.12 \pm 124.42^{+}$ | $1459.61 \pm 176.68^{+}$ | $743.39 \pm 104.30^{+}$ | $0.48 \pm 0.04$ |
| **Striatum** | SBR | MD ($x10^3$ $mm^2/s$) | AD ($x10^3$ $mm^2/s$) | RD ($x10^3$ $mm^2/s$) | FA ($mm^2/s$) |
| HC | - | 745.27 ± 67.02 | $968.49 \pm 81.79^{*}$ | $690.48 \pm 156.01^{*}$ | $0.24 \pm 0.03^{*}$ |
| RBD | $1.60 \pm 0.13^{*}$ | 743.14 ± 44.17 | 990.99 ± 75.03 | $622.19 \pm 45.06^{*}$ | $0.26 \pm 0.03^{*}$ |
| PD | $1.35 \pm 0.16^{*}$ | 772.75 ± 78.85 | $1023.80 \pm 91.80^{*}$ | 653.29 ± 79.10 | 0.25 ± 0.03 |

AD, axial diffusivity; FA, fractional anisotropy; HC, healthy control; MD, mean diffusivity; PD, Parkinson's disease; RBD, rapid eye movement sleep behavior disorder; RD, radial diffusivity; SBR, specific-binding ratio; SNpc, substantia nigra pars compacta.

**SNpc:** ∗ and + = significant difference at $p < 0.05$ for subgroup analysis using analysis of variance with Tukey's post hoc test for intergroup differences of all groups.

**Striatum**: ∗ = significant difference at $p < 0.05$ for subgroup analysis using analysis of variance with Tukey's post hoc test for intergroup differences of all groups or the Mann–Whitney U test for intergroup differences between the RBD and PD groups.

Figure 3. Neuromelanin and diffusion tensor values of the SNpc for each of the HC, RBD, and PD groups. ∗=significant difference at $p < 0.05$ for subgroup analysis using analysis of variance with Tukey's post hoc test for intergroup differences of all groups. AD, axial diffusivity; FA, fractional anisotropy; HC, healthy control; MD, mean diffusivity; PD, Parkinson's disease; RBD, rapid eye movement sleep behavior disorder; RD, radial diffusivity; SNpc, substantia nigra pars compacta

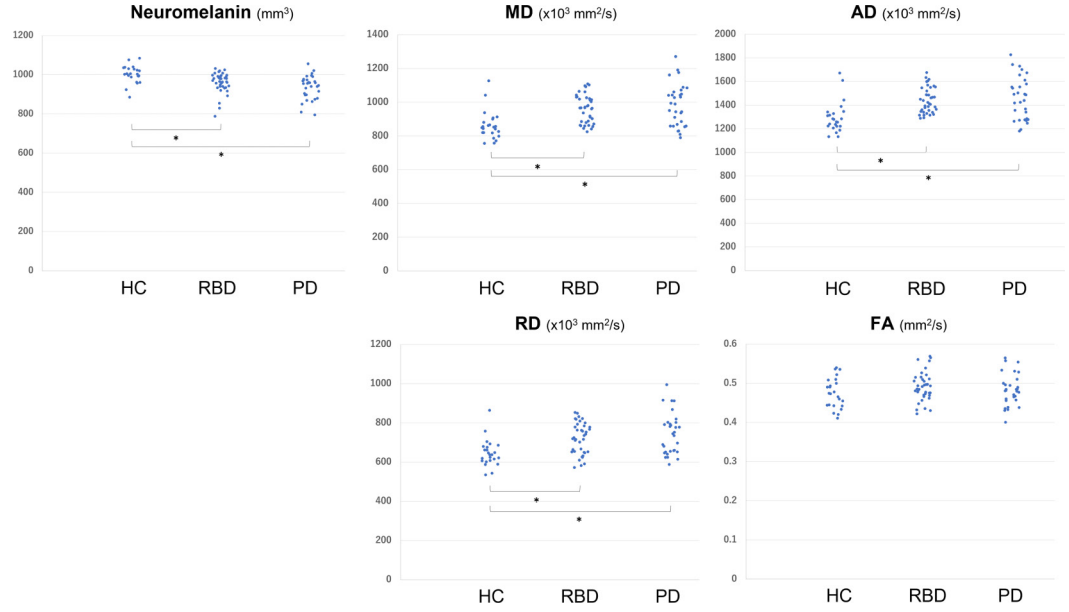


the RBD and PD groups. For the striatum, the AUC for the SBR for discriminating PD from RBD was 0.87 [95% CI: 0.73 to 0.95]. The AUC for the striatum diffusion tensor values was not calculated because these values did not differ more significantly than the SNpc values among the groups.

## DISCUSSION

A morphological and neurochemical correlative study has reported that 40–70% of dopaminergic neurons in the SN are already lost at the time of clinical onset of PD.[18] Therefore, assessing the sequential changes in dopamine neurons in the

Figure 4. Diffusion tensor values and the SBR of the striatum for each of the HC, RBD, and PD groups. ∗=significant difference at $p < 0.05$ for subgroup analysis using analysis of variance with Tukey's post hoc test for intergroup differences of all groups or the Mann–Whitney *U* test for intergroup differences between the RBD and PD groups. AD, axial diffusivity; FA, fractional anisotropy; HC, healthy control; MD, mean diffusivity; PD, Parkinson's disease; RBD, rapid eye movement sleep behavior disorder; RD, radial diffusivity; SBR, specific binding ratio; SNpc, substantia nigra pars compacta

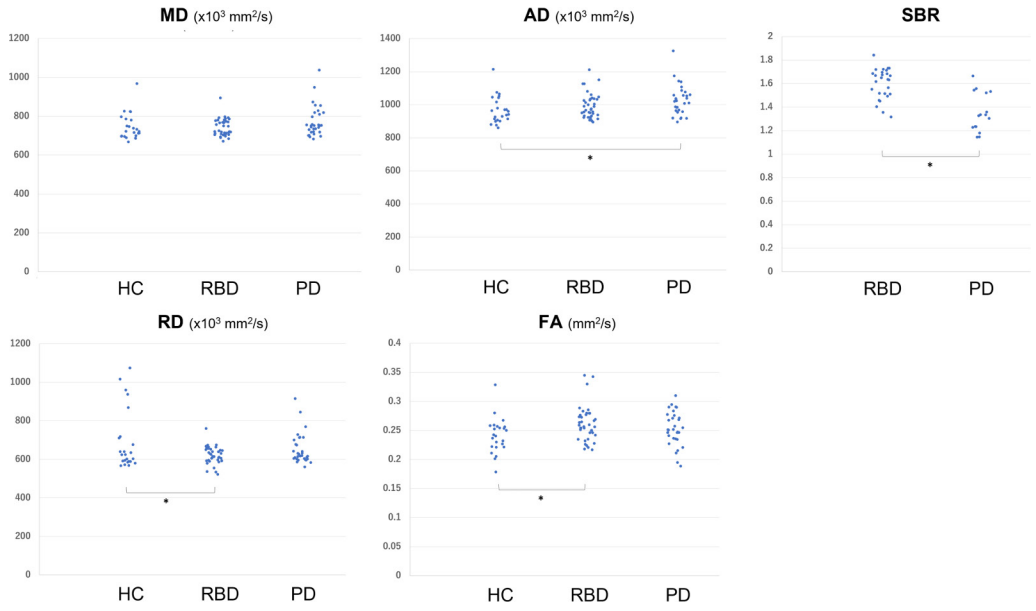

Figure 5. AUC for each SNpc and striatum value. AD, axial diffusivity; AUC, area under the receiver-operating characteristic curve; DAT-SPECT, dopamine transporter single photon emission computed tomography; DTI, diffusion tensor imaging; FA, fractional anisotropy; HC, healthy control; MD, mean diffusivity; PD, Parkinson's disease; RBD, rapid eye movement sleep behavior disorder; RD, radial diffusivity; SBR, specific binding ratio; SNpc, substantia nigra pars compacta.

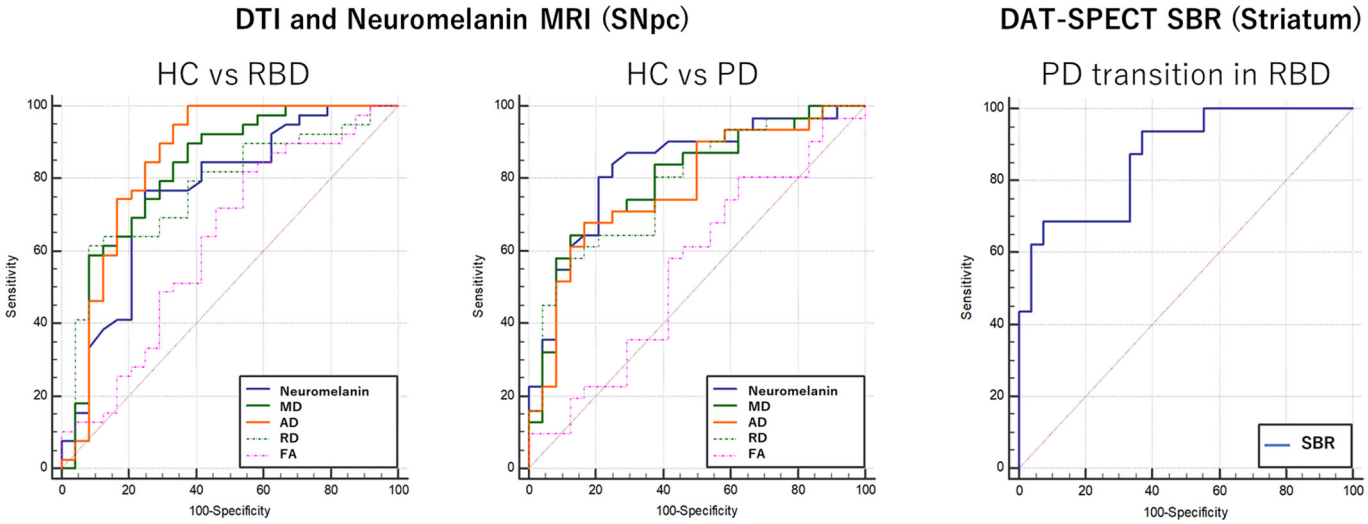


SNpc during the preclinical phase of PD is important for early diagnosis prior to symptom onset. Because most patients with RBD are in the prodromal phase of PD, damage to the SN should be evident. Significant decreases in the neuromelanin-sensitive volume and signal intensity in the SN of patients with RBD have been reported.[6]

The present neuromelanin MRI results suggest that significant dopamine neuron loss occurs in the SNpc during RBD development in healthy people, but that subsequent minimum dopamine neuron loss occurs in the SNpc during the time course of RBD and the transition from RBD to PD. This concept is supported by the finding that MD showed the same tendency throughout the early stage of PD development, reflecting the cellular density. Other diffusion tensor values, including AD and RD, showed the same tendency. These results suggest that neuromelanin MRI and DTI may be useful in the diagnosis of RBD and early PD. In contrast, FA was not useful for evaluating RBD or PD, in agreement with the results of a previous study that found that measuring FA in the SN was not useful for PD diagnosis.[19] Meanwhile, striatal DTI that shows microstructural changes in the striatum is not superior to SNpc DTI or neuromelanin MRI in evaluating the preclinical phase of PD. In some of the striatum DTI values, significant intergroup differences were found, but the tendencies of values varied during disease development. This may be due to the heterogeneity of neuronal changes in the striatum.

Meanwhile, we consider that evaluation of the early transition of PD in patients with idiopathic RBD by discriminating PD from RBD is important, because most patients with idiopathic RBD develop synucleinopathy associated with diseases such as PD and DLB.[3,20] However, since the interval between the diagnosis of RBD and the clinical diagnosis of synucleinopathy averages 14 years, while the range has extended to 29 years,[20] a quantitative marker is required to identify the development of synucleinopathy in patients with idiopathic RBD. The present results showed no apparent tendency in SNpc or striatum values during the time course of RBD, and no significant differences in neuromelanin or diffusion tensor values between RBD and PD. A previous study using transcranial sonography also showed that the area of echogenicity of the SN did not change during the time course of RBD, even in patients with the transition to PD.[16] Therefore, we consider that the SNpc by itself is not a marker for the transition to PD in RBD. In contrast, the significant decrease in DAT-SPECT SBR in PD compared with RBD indicates that DAT-SPECT may be useful for evaluating the transition to PD in RBD, which agrees with a previous report.[21]

During disease development, although a significant correlation between the SNpc and the striatum in terms of most diffusion tensor values for all groups combined in the present study indicates the structural connectivity of the nigrostriatal pathway between the SNpc and the striatum, asynchrony of changes in dopamine neuron loss versus striatal dysfunction was indicated in another study that assessed the relationship between the SNpc and the striatum within the nigrostriatal system using neuromelanin MRI and striatal DAT imaging.[22] There was a significant but not very strong correlation within the nigrostriatal system between dopamine neuronal changes in the SNpc and the striatum in all of the present subjects, including healthy people and patients with RBD and early PD. In contrast, a previous study showed that dopamine neuron loss in the SNpc correlated strongly with presynaptic dopamine neuronal dysfunction in patients with synucleinopathy.[23] These findings suggest that there may be a difference in the relationship between the SNpc and the striatum between the development of RBD and the transition to synucleinopathy such as PD in RBD. Therefore, there appears to be a difference in the roles of the SNpc and the striatum in disease development.

We consider that, in the SNpc, dopamine neuron loss plays an important role in RBD development and leads to subsequent depletion of presynaptic nerve terminals in the striatum. In presynaptic nerve terminals, the loss of nigrostriatal projections is presumed to cause PD-related motor symptoms.[24] As a pathological mechanism, the aggregation of presynaptic protein α-synuclein has been shown to be the major component in the accumulation of Lewy bodies and neurites, which may play an important role in the etiopathogenesis of PD.[25] Lewy neurites are found more abundantly and earlier in the distal axons and may impair retrograde axonal transport, leading to neuronal loss.[26] Based on these findings, the loss of nigrostriatal projections may play an important role in the transition to PD in RBD, and then a dying-back process begins from the presynaptic terminals and extends toward the SNpc. Furthermore, a recent nuclear imaging study of the presynaptic terminals showed that the loss of DAT in the striatum exceeded the loss in the SN in patients with early PD.[27] One explanation for this finding relates to evidence suggesting that distal axonal degeneration occurs initially before proceeding retrograde towards the cell body[28]; accordingly, striatal functional neuroimaging such as DAT-SPECT may provide quantitative markers for monitoring the transition to PD in RBD.

The present study has some limitations. First, whether all subjects in the RBD group will develop PD is unknown. Additional longitudinal follow-up is needed. However, because patients in the PD group had a history of probable RBD, it may be possible to evaluate sequential changes in the nigrostriatal system during the entire preclinical phase of PD. Second, there was a lack of DAT-SPECT data in the HC group because of the difficulty of performing DAT-SPECT in healthy volunteers. Since a previous study reported the utility of striatal DAT imaging for monitoring the progression of RBD in healthy people,[11] DAT-SPECT may have performance sufficient to enable evaluation of the entire preclinical phase of PD. Third, only 60% (9/15) of the subjects in the RBD group underwent DAT-SPECT. Acknowledging this, all DAT-SPECT data of idiopathic RBD subjects were included as the RBD group in the analysis of the present study. Because no significant sequential difference of the SN in RBD subjects was reported in a longitudinal study,[16] the present results also showed no apparent tendencies of both the SNpc and the striatum in the RBD group.

## CONCLUSION

Quantification of the SNpc and the striatum using MRI and DAT-SPECT may show the mechanism of neurodegenerative changes within the nigrostriatal system during the preclinical phase of PD. Accordingly, as an imaging biomarker, quantifying changes in the SNpc with MRI can provide useful diagnostic information for both RBD and early PD, and quantifying changes in the striatum with DAT-SPECT can provide useful diagnostic information for the transition to PD in RBD.

## REFERENCES


1. Tolosa E, Gaig C, Santamaría J, Compta Y. Diagnosis and the premotor phase of Parkinson disease. *Neurology* 2009; **72**(7 Suppl): S12–20. doi: https://doi.org/10.1212/WNL.0b013e318198db11
2. Iranzo A, Santamaria J, Tolosa E. The clinical and pathophysiological relevance of REM sleep behavior disorder in neurodegenerative diseases. *Sleep Med Rev* 2009; **13**: 385–401. doi: https://doi.org/10.1016/j.smrv.2008.11.003
3. Iranzo A, Lomeña F, Stockner H, Valldeoriola F, Vilaseca I, Salamero M, et al. Decreased striatal dopamine transporter uptake and substantia nigra hyperechogenicity as risk markers of synucleinopathy in patients with idiopathic rapid-eye-movement sleep behaviour disorder: a prospective study [corrected]. *Lancet Neurol* 2010; **9**: 1070–7. doi: https://doi.org/10.1016/S1474-4422(10)70216-7
4. Sasaki M, Shibata E, Tohyama K, Takahashi J, Otsuka K, Tsuchiya K, et al. Neuromelanin magnetic resonance imaging of locus ceruleus and substantia nigra in Parkinson's disease. *Neuroreport* 2006; **17**: 1215–8. doi: https://doi.org/10.1097/01.wnr.0000227984.84927.a7
5. Ohtsuka C, Sasaki M, Konno K, Koide M, Kato K, Takahashi J, et al. Changes in substantia nigra and locus coeruleus in patients with early-stage Parkinson's disease using neuromelanin-sensitive MR imaging. *Neurosci Lett* 2013; **541**: 93–8. doi: https://doi.org/10.1016/j.neulet.2013.02.012
6. Pyatigorskaya N, Gaurav R, Arnaldi D, Leu-Semenescu S, Yahia-Cherif L, Valabregue R, et al. Magnetic resonance imaging biomarkers to assess substantia nigra damage in idiopathic rapid eye movement sleep behavior disorder. *Sleep* 2017; **40**01 11 2017. doi: https://doi.org/10.1093/sleep/zsx149
7. Unger MM, Belke M, Menzler K, Heverhagen JT, Keil B, Stiasny-Kolster K, et al. Diffusion tensor imaging in idiopathic REM sleep behavior disorder reveals microstructural changes in the brainstem, substantia nigra, olfactory region, and other brain regions. *Sleep* 2010; **33**: 767–73. doi: https://doi.org/10.1093/sleep/33.6.767
8. Kamagata K, Hatano T, Okuzumi A, Motoi Y, Abe O, Shimoji K, et al. Neurite orientation dispersion and density imaging in the substantia nigra in idiopathic Parkinson disease. *Eur Radiol* 2016; **26**: 2567–77. doi: https://doi.org/10.1007/s00330-015-4066-8
9. Andica C, Kamagata K, Hatano T, Okuzumi A, Saito A, Nakazawa M, et al. Neurite orientation dispersion and density imaging of the nigrostriatal pathway in Parkinson's disease: retrograde degeneration observed by tract-profile analysis. *Parkinsonism Relat Disord* 2018; **51**: 55–60. doi: https://doi.org/10.1016/j.parkreldis.2018.02.046
10. Brooks DJ, Pavese N. Imaging biomarkers in Parkinson's disease. *Prog Neurobiol* 2011; **95**: 614–28. doi: https://doi.org/10.1016/j.pneurobio.2011.08.009
11. Iranzo A, Valldeoriola F, Lomeña F, Molinuevo JL, Serradell M, Salamero M, et al. Serial dopamine transporter imaging of nigrostriatal function in patients with idiopathic rapid-eye-movement sleep behaviour disorder: a prospective study. *Lancet Neurol* 2011; **10**: 797–805. doi: https://doi.org/10.1016/S1474-4422(11)70152-1
12. Hughes AJ, Daniel SE, Kilford L, Lees AJ. Accuracy of clinical diagnosis of idiopathic Parkinson's disease: a clinico-pathological study of 100 cases. *J Neurol Neurosurg Psychiatry* 1992; **55**: 181–4. doi: https://doi.org/10.1136/jnnp.55.3.181

13. Hoehn MM, Yahr MD. Parkinsonism: onset, progression and mortality. *Neurology* 1967; **17**: 427–42. doi: https://doi.org/10.1212/WNL.17.5.427
14. Miyamoto T, Miyamoto M, Iwanami M, Kobayashi M, Nakamura M, Inoue Y, et al. The REM sleep behavior disorder screening questionnaire: validation study of a Japanese version. *Sleep Med* 2009; **10**: 1151–4. doi: https://doi.org/10.1016/j.sleep.2009.05.007
15. American Academy of Sleep Medicine.*International Classification of Sleep Disorders (ICSD)*. Third Edition. Westchester, Ill: American Academy of Sleep Medicine; 2014.
16. Iranzo A, Stockner H, Serradell M, Seppi K, Valldeoriola F, Frauscher B, et al. Five-year follow-up of substantia nigra echogenicity in idiopathic REM sleep behavior disorder. *Mov Disord* 2014; **29**: 1774–80. doi: https://doi.org/10.1002/mds.26055
17. Jenkinson M, Beckmann CF, Behrens TEJ, Woolrich MW, Smith SM. FSL. *Neuroimage* 2012; **62**: 782–90. doi: https://doi.org/10.1016/j.neuroimage.2011.09.015
18. Bernheimer H, Birkmayer W, Hornykiewicz O, Jellinger K, Seitelberger F. Brain dopamine and the syndromes of Parkinson and Huntington. Clinical, morphological and neurochemical correlations. *J Neurol Sci* 1973; **20**: 415–55. doi: https://doi.org/10.1016/0022-510X(73)90175-5
19. Hirata FCC, Sato JR, Vieira G, Lucato LT, Leite CC, Bor-Seng-Shu E, et al. Substantia nigra fractional anisotropy is not a diagnostic biomarker of Parkinson's disease: a diagnostic performance study and meta-analysis. *Eur Radiol* 2017; **27**: 2640–8. doi: https://doi.org/10.1007/s00330-016-4611-0
20. Schenck CH, Boeve BF, Mahowald MW. Delayed emergence of a parkinsonian disorder or dementia in 81% of older men initially diagnosed with idiopathic rapid eye movement sleep behavior disorder: a 16-year update on a previously reported series. *Sleep Med* 2013; **14**: 744–8. doi: https://doi.org/10.1016/j.sleep.2012.10.009
21. Iranzo A, Santamaría J, Valldeoriola F, Serradell M, Salamero M, Gaig C, et al. Dopamine transporter imaging deficit predicts early transition to synucleinopathy in idiopathic rapid eye movement sleep behavior disorder. *Ann Neurol* 2017; **82**: 419–28. doi: https://doi.org/10.1002/ana.25026
22. Martín-Bastida A, Lao-Kaim NP, Roussakis AA, Searle GE, Xing Y, Gunn RN, et al. Relationship between neuromelanin and dopamine terminals within the Parkinson's nigrostriatal system. *Brain* 2019; **142**: 2023–36. doi: https://doi.org/10.1093/brain/awz120
23. Kuya K, Shinohara Y, Miyoshi F, Fujii S, Tanabe Y, Ogawa T. Correlation between neuromelanin-sensitive MR imaging and (123)I-FP-CIT SPECT in patients with parkinsonism. *Neuroradiology* 2016; **58**: 351–6. doi: https://doi.org/10.1007/s00234-016-1644-7
24. Burke RE, O'Malley K. Axon degeneration in Parkinson's disease. *Exp Neurol* 2013; **246**: 72–83. doi: https://doi.org/10.1016/j.expneurol.2012.01.011
25. Braak H, Sandmann-Keil D, Gai W, Braak E. Extensive axonal Lewy neurites in Parkinson's disease: a novel pathological feature revealed by alpha-synuclein immunocytochemistry. *Neurosci Lett* 1999; **265**: 67–9. doi: https://doi.org/10.1016/S0304-3940(99)00208-6
26. Perlson E, Maday S, Fu M-M, Moughamian AJ, Holzbaur ELF. Retrograde axonal transport: pathways to cell death? *Trends Neurosci* 2010; **33**: 335–44. doi: https://doi.org/10.1016/j.tins.2010.03.006
27. Caminiti SP, Presotto L, Baroncini D, Garibotto V, Moresco RM, Gianolli L, et al. Axonal damage and loss of connectivity in nigrostriatal and mesolimbic dopamine pathways in early Parkinson's disease. *Neuroimage Clin* 2017; **14**: 734–40. doi: https://doi.org/10.1016/j.nicl.2017.03.011
28. Tagliaferro P, Burke RE. Retrograde axonal degeneration in Parkinson disease. *J Parkinsons Dis* 2016; **6**: 1–15. doi: https://doi.org/10.3233/JPD-150769